Networks and Heterogeneous Media

http://www.aimspress.com/journal/nhm

NHM, 18(3): 1178–1189.
DOI: 10.3934/nhm.2023050
Received: 18 December 2022
Revised: 26 February 2023
Accepted: 09 March 2023
Published: 06 April 2023

Research article

A novel error analysis of nonconforming finite element for the clamped Kirchhoff plate with elastic unilateral obstacle

Lifang Pei, Man Zhang and Meng Li*

School of Mathematics and Statistics, Zhengzhou University, Zhengzhou 450001, P.R China

* **Correspondence:** Email: limeng@zzu.edu.cn.

Abstract: A nonconforming finite element method (FEM) is proposed and analyzed for the clamped thin elastic Kirchhoff plate unilaterally constrained by an elastic obstacle. The discrete scheme is constructed by using the strongly discontinuous Bergan's energy-orthogonal plate element, which has simple degrees of freedom and about 25 percent fewer global dimension than that of the famous triangular Morley element. A novel error analysis is presented to overcome the difficulties caused by the strong discontinuity and derive the optimal estimate. Numerical experiments are carried out to verify the theoretical analysis.

Keywords: elastic obstacle; kirchhoff plate; nonconforming FEM; Bergan's element; optimal error estimate

1. Introduction

Let $\Omega \subset \mathbb{R}^2$ be a bounded convex polygonal domain covered by a thin flat plate, and $\Gamma = \partial\Omega$ be the Lipschitz continuous boundary of Ω. For a given loading function $f \in L^2(\Omega)$, $f \leq 0$ *a.e.* in Ω, and an elastic obstacle $\psi \in L^2(\Omega)$, we consider the following clamped Kirchhoff plate problem with elastic unilateral obstacle (refer to [1, 2]):

$$\begin{cases} \text{Find } u \in V, \text{ such that} \\ J(u) \leq J(v), \quad \forall v \in V, \end{cases} \tag{1.1}$$

where

$$V = H_0^2(\Omega), \quad J(v) = \frac{1}{2}a(v,v) + \frac{1}{2}j(v) - (f,v),$$

$$a(w,v) = \int_\Omega [\Delta w \Delta v + (1-\nu)(2w_{xy}v_{xy} - w_{xx}v_{yy} - w_{yy}v_{xx})]dxdy, \quad \forall w, v \in V,$$

$$j(v) = \int_\Omega \kappa[(v-\psi)_-]^2 dxdy, \qquad (f,v) = \int_\Omega fv dxdy.$$

Here $J(v)$ is the total energy, $a(v,v)$ represents the strain energy corresponding to displacement v of the plate, $j(v)$ can be interpreted as the contribution from the contact with ψ and (f,v) is the potential energy. Moreover, the symbol $v_- = \min\{v,0\}$, $\nu \in (0,1/2)$ is the Poisson's ratio, $\kappa \in L^\infty(\Omega)$ describes the stiffness of the obstacle and satisfies $\kappa \geq \kappa_0 > 0$ *a.e.* in Ω. In the limiting case $\kappa \to \infty$, the obstacle becomes rigid and the problem (1.1) reduces to a constrained minimisation:

$$\begin{cases} \text{Find } u \in K^*, \text{ such that} \\ u = \arg\min\limits_{v\in K^*}[\dfrac{1}{2}a(v,v) - (f,v)] \end{cases} \tag{1.2}$$

with $K^* = \{v \in V : v \geq \psi \text{ in } \Omega\}$. (1.2) is a classical displacement obstacle model of clamped Kirchhoff plate (cf. [3]) and equivalent to a fourth-order variational inequality:

$$\begin{cases} \text{Find } u \in K^*, \text{ such that} \\ a(u, v-u) \geq (f, v-u), \quad \forall v \in K^*. \end{cases} \tag{1.3}$$

Different with the displacement obstacle model (1.2), the elastic obstacle problem (1.1) can be investigated based on the following weak formulation [1]:

$$\text{Find } u \in V, \text{ such that } a(u,v) + \int_\Omega \kappa(u-\psi)_- v dxdy = (f,v), \quad \forall v \in V, \tag{1.4}$$

which has a unique solution [2] and is equivalent to another fourth-order variational inequality:

$$\begin{cases} \text{Find } u \in V, \text{ such that } \forall v \in V \\ a(u, v-u) + \displaystyle\int_\Omega \frac{\kappa}{2}[(v-\psi)_-]^2 dxdy - \int_\Omega \frac{\kappa}{2}[(u-\psi)_-]^2 dxdy \geq (f, v-u). \end{cases} \tag{1.5}$$

As we all know, analytical solutions to obstacle problems are always difficult to obtain. In this case, the study of numerical solutions has attracted a lot of attention. The finite element method (FEM) is a popular numerical method to solve obstacle problems [3–8]. In the last decades, more efforts have devoted to FEM analysis for the limit form of elastic obstacle problem (1.1), i.e., displacement obstacle problem (1.2), see [9–17] and references therein. But works focusing on FEMs of the elastic obstacle problem (1.1) are relatively rather few in the existing literature. From [1], the convergence analysis of a mixed FEM for the elastic obstacle problem (1.1) was obtained, where elements employed must satisfy C^0 continuous. In [18], a stabilized FEM was constructed for (1.1) with a C^1 continuous requirement. [2] provided a general framework of optimal error estimates for FEM, where the continuous requirement is relatively relaxed but continuity at each element's vertex of the subdivision is indispensable. In this situation, a natural question is whether these requirements for continuity can be completely removed. In other words, a key difficulty is how to get the optimal error estimates for a strongly discontinuous element dissatisfying above continuity requirements, which is just the motivation of this work.

In this paper, as an attempt, we will investigate the FEM approximation for the elastic obstacle problem (1.1) by using Bergan's energy-orthogonal element. This element is constructed through an

energy-orthogonal free formulation (cf. [19, 20]), which is convergent for arbitrary meshes. Its degrees of freedom are all defined on the element's vertex, including the function values and the two first derivatives at the three vertices of each element, which are very simple and can be used conveniently. Moreover, the global dimension of the vector of unknowns is only $3NP$ (NP denotes the number of vertex in mesh subdivision), about 25 percent fewer than that of the famous triangular Morley element (about $4NP$). This property is very useful for a reduction the amount of computation. But the element has strong discontinuous, that is, the shape function and its first derivatives are no longer continuous at the element's the vertex. This element does not satisfy the above mentioned continuity requirements. Despite so high discontinuity, Bergan's energy-orthogonal plate element has been applied to the FEM approximate for the displacement obstacle problem (1.2) (see [12]). The authors developed a convergence analysis method and obtained the optimal error estimate of order $O(h)$ in [12]. We note that the convergence analysis relied on two additional introduced tools, i.e., an approximation subset and an enriching operator from Bergan's energy-orthogonal FE space to C^1-conforming Bell FE space and the process is very complicated.

This paper aims to develop a new error analysis of Bergan's energy-orthogonal element approximation for the elastic obstacle problem (1.1). Unlike the convergence analysis in [12], we make full use of some special approaches, including interpolation operator splitting and energy orthogonality, to derive the optimal error estimates of order $O(h)$ in the broken energy norm. The theoretical analysis is very simple and clear. The numerical results demonstrate the proposed method not only enjoys one-order accuracy but also can well reflect the influence brought by the obstacle stiffness parameter κ.

The organization of this paper is as follows: In Section 2, Bergan's energy-orthogonal plate element and its typical properties are briefly introduced. Then we propose a novel error analysis approach and obtain the optimal error estimate of order $O(h)$ successfully in Section 3. At last, Section 4 provides some numerical results to illustrate the validity of the theoretical analysis.

2. The Bergan's energy-orthogonal plate element approximation scheme

Bergan's energy-orthogonal element was first proposed by Bergan et al. in [19] using the free formulation scheme. Then Shi et al. [20] proved that this element is equivalent to a nonconforming element constructed based on a specific interpolation Π_K (see Eq (2.3) below), where Π_K is introduced to form the shape function. It is shown in [20] that the special construction of interpolation Π_K makes the two components of the shape function energy-orthogonal and the stiffness matrix consistent with that in the free formulation scheme. In the following, we will introduce Bergan's energy-orthogonal plate element briefly, and the readers can refer to [19, 20] for details.

Assume that T_h is a regular triangulation of Ω with mesh size h. For a given $K \in T_h$, let its diameter be h_K, three vertices be $p_i(x_i, y_i)$ and the area coordinates be λ_i for $i = 1, 2, 3$. Firstly, we select nine nodal parameters set as $\Sigma(v) = \{v_1, v_{1x}, v_{1y}, v_2, v_{2x}, v_{2y}, v_3, v_{3x}, v_{3y}\}$, where $v_i = v(p_i)$, $v_{ix} = \frac{\partial v}{\partial x}(p_i)$, $v_{iy} = \frac{\partial v}{\partial y}(p_i)$, $i = 1, 2, 3$. The shape function space is taken as same as that of Zienkiewicz element, i.e., $\widetilde{P}(K) = span\{\widetilde{N}_1, \widetilde{N}_2, \cdots, \widetilde{N}_9\}$, here $\widetilde{N}_j = \lambda_j$, $\widetilde{N}_{4+j} = \lambda_j\lambda_{j+1}$, $\widetilde{N}_{6+j} = \lambda_j^2\lambda_{j+1} - \lambda_{j+1}\lambda_j^2$, $j = 1, 2, 3$ and

$\lambda_4 = \lambda_1$. Then the associated conventional interpolation operator $\widetilde{\Pi}_K : H^3(K) \to \widetilde{P}(K)$ satisfies

$$\widetilde{\Pi}_K v = \sum_{i=1}^{6} \alpha_i(v)\widetilde{N}_i + \sum_{i=7}^{9} \alpha_i(v)\widetilde{N}_i \triangleq \overline{r}_K(v) + r'_K(v), \quad \forall v \in H^3(K), \tag{2.1}$$

where $\overline{r}_K(v)$ and $r'_K(v)$ are the quadratic and cubic terms respectively, and the coefficients $\alpha_i(v)$ can be written as: $\alpha_j(v) = v_j$, $\alpha_{3+j}(v) = \frac{c_{(j+2)}}{2}(v_{jx} - v_{(j+1)x}) - \frac{b_{(j+2)}}{2}(v_{jy} - v_{(j+1)y})$, $\alpha_{6+j}(v) = v_j - v_{(j+1)} + \frac{c_{(j+2)}}{2}(v_{jx} + v_{(j+1)x}) - \frac{b_{(j+2)}}{2}(v_{jy} + v_{(j+1)y})$ with $b_j = y_{(j+1)} - y_{(j+2)}$ and $c_j = -(x_{(j+1)} - x_{(j+2)})$ for $j = 1, 2, 3$, here and later subscripts $(j + i)$ will be replaced with $(j + i)(mod\ 3)$ when $(j + i) > 3$ for $i = 1, 2$.

Next we introduce another shape function space $P(K) = span\{N_1, N_2, \cdots, N_9\}$, where $N_i = \widetilde{N}_i$, $i = 1, 2, \cdots, 6$, $N_{6+j} = (\lambda_j - \lambda_{(j+1)})^3$, $j = 1, 2, 3$ and $\lambda_4 = \lambda_1$. It is easy to verify that

$$\int_K \partial_{xx} N_i dxdy = \int_K \partial_{yy} N_i dxdy = \int_K \partial_{xy} N_i dxdy = 0, \ i = 7, 8, 9, \tag{2.2}$$

and the associated traditional interpolation operator $\hat{\Pi}_K : H^3(K) \to P(K)$ is defined by

$$\hat{\Pi}_K v = \sum_{i=1}^{6} \beta_i(v) N_i + \sum_{i=7}^{9} \beta_i(v) N_i \triangleq \overline{S}_K(v) + S'_K(v), \quad \forall v \in H^3(K), \tag{2.3}$$

where $\beta_i(v)$, $i = 1, 2, ..., 9$, can be expressed as:

$$\begin{aligned}
\beta_j(v) &= \frac{13}{9} v_j - \frac{2}{9}(v_{(j+1)} + v_{(j+2)}) + \frac{1}{9}[(c_{(j+2)} - c_{(j+1)})v_{jx} + c_{(j+2)}v_{(j+1)x} - c_{(j+1)}v_{(j+2)x}] \\
&\quad + \frac{1}{9}[(b_{(j+1)} - b_{(j+2)})v_{jy} - b_{(j+2)}v_{(j+1)y} + b_{(j+1)}v_{(j+2)y}], \\
\beta_{3+j}(v) &= -\frac{1}{3}(v_j + v_{(j+1)} - 2v_{(j+2)}) + \frac{1}{6}[(2c_{(j+2)} - c_j)v_{jx} + (c_{(j+1)} - 2c_{(j+2)})v_{(j+1)x} \\
&\quad + (c_{(j+1)} - c_j)v_{(j+2)x}] + \frac{1}{6}[(b_j - 2b_{(j+2)})v_{jy} + (2b_{(j+2)} - b_{(j+1)})v_{(j+1)y} + (b_j - b_{(j+1)})v_{(j+2)y}], \\
\beta_{6+j}(v) &= -\frac{2}{9}(v_j - v_{(j+1)}) + \frac{1}{54}[(c_j - 6c_{(j+2)})v_{jx} + (c_{(j+1)} - 6c_{(j+2)})v_{(j+1)x} + c_{(j+2)}v_{(j+2)x}] \\
&\quad + \frac{1}{54}[(6b_{(j+2)} - b_j)v_{jy} + (6b_{(j+2)} - b_{(j+1)})v_{(j+1)y} - b_{(j+2)}v_{(j+2)y}],
\end{aligned}$$

for $j = 1, 2, 3$.

Now employing Eq (2.1) and Eq (2.3), we introduce an interpolation operator Π_K as

$$\Pi_K : H^3(K) \to P(K), \quad \Pi_K v = \overline{r}_K(v) + S'_K(v), \ \forall\, v \in H^3(K). \tag{2.4}$$

Then taking $\Pi_K v$ as the shape function on K and $\Sigma(v)$ as its associated nodal parameters (vanishing at nodes on the boundary Γ), and defining an interpolation operator Π_h for every $v \in H^3(\Omega)$ with $(\Pi_h v)|_K = \Pi_K v$, we can obtain a piecewise cubic polynomial space on Ω denoted by V_h. It has been shown in [20] that V_h is equivalent to the Bergan's energy-orthogonal plate element first proposed by Bergan etal through the free formulation scheme. Obviously, the construction process of V_h is quite different from conventional element spaces. Herein the shape function on K is formulated through the operator Π_K involving two interpolation operators $\widetilde{\Pi}_K$ and $\hat{\Pi}_K$.

It follows from Eqs (2.1), (2.4) and the formulas of $\alpha_i(v)$ and $\beta_i(v)$ $(i = 1, 2, \cdots, 9)$ that

$$\Pi_K v(p_j) - v_j = \beta_{6+j}(v) - \beta_{6+(j+2)}(v),$$

$$\begin{aligned}
&\frac{\partial \Pi_K v}{\partial x}(p_j) - v_{jx} \\
&= \frac{1}{2\triangle}[3(b_j - b_{(j+1)})\beta_{6+j}(v) + 3(b_{(j+2)} - b_j)\beta_{6+(j+2)}(v) - b_{(j+1)}\alpha_{6+j}(v) + b_{(j+2)}\alpha_{6+(j+2)}(v)], \\
&\frac{\partial \Pi_K v}{\partial y}(p_j) - v_{jy} \\
&= \frac{1}{2\triangle}[3(c_j - c_{(j+1)})\beta_{6+j}(v) + 3(c_{(j+2)} - c_j)\beta_{6+(j+2)}(v) - c_{(j+1)}\alpha_{6+j}(v) + c_{(j+2)}\alpha_{6+(j+2)}(v)]
\end{aligned} \tag{2.5}$$

for $j = 1, 2, 3,$ where $\triangle$ represents the area of K. Thus $\Pi_K v$ and its two first derivatives are discontinuous at vertices p_j $(j = 1, 2, 3)$. Moreover, the mean value of $\Pi_K v$ along the element's each edge F can be calculated as

$$\frac{1}{|F|}\int_F \Pi_K v ds = \frac{1}{|F|}\int_F (\overline{r}_K(v) + S'_K(v))ds = \frac{1}{|F|}\int_F \overline{r}_K(v)ds + \frac{1}{4}(\beta_7(v) - \beta_9(v)).$$

Obviously, it is not continuous neither. In spite of so high discontinuity of the interpolation $\Pi_K v$, the element space possesses the following special features (cf. [20]), which will play an important role in the follow-up convergence analysis.

Lemma 2.1. ($\mathcal{R}1$) *For any $v_h \in V_h$, there exists a $v \in H^3(K)$ such that*

$$v_h|_K = \Pi_K v,\ v_h = \bar{v}_h + v'_h,\ \bar{v}_h|_K = \overline{r}_K(v),\ v'_h|_K = S'_K(v). \tag{2.6}$$

When $v_h|_K \in \mathbb{P}_2(K)$, there holds $v_h = \bar{v}_h$. Moreover, $\partial_{xx}\overline{r}_K(v)$, $\partial_{xy}\overline{r}_K(v)$ and $\partial_{yy}\overline{r}_K(v)$ are constants, which together with Eq (2.2) *imply that $\overline{r}_K(v)$ and $S'_K(v)$ are energy-orthogonal, thus the element is called energy-orthogonal. Let $\nabla^2 v_h$ be the Hessian matrix of v_h, then we have $\int_K \nabla^2\bar{v}_h : \nabla^2 v'_h dxdy = 0$.*
($\mathcal{R}2$) *For $j = 1, 2, 3$, the quadratic term $\overline{r}_K(v)$ satisfies*

$$\overline{r}_K(v)(p_j) = v_j, \tag{2.7}$$

$$\overline{r}_K(v)(\frac{p_j + p_{(j+1)}}{2}) = \frac{v_j + v_{(j+1)}}{2} + \frac{(v_{jx} - v_{(j+1)x})c_{(j+2)}}{8} - \frac{(v_{jy} - v_{(j+1)y})b_{(j+2)}}{8}, \tag{2.8}$$

i.e., for any $v_h \in V_h$, its quadratic term $\bar{v}_h$ is continuous at the element's vertices and midpoints of edges. In other words, $\bar{v}_h \in C^0(\Omega)$.
($\mathcal{R}3$) *For any $v \in H^3(K)$ and integer m $(0 \le m \le 3)$, there holds*

$$|v - \Pi_K(v)|_{m,K} + |v - \overline{r}_K(v)|_{m,K} \le Ch_K^{3-m}|v|_{3,K}, \tag{2.9}$$

$$\left|r'_K(v)\right|_{m,K} + \left|S'_K(v)\right|_{m,K} \le Ch_K^{3-m}|\Pi_K v|_{3,K}. \tag{2.10}$$

Here and later, C denotes a positive constant independent of h and may be different at each appearance.

We consider the Bergan's energy-orthogonal plate element discrete approximation form of the variational inequality (1.5) as:

$$\begin{cases} \text{Find } u_h \in V_h, \text{ such that } \forall v_h \in V_h \\ a(u_h, v_h - u_h) + \sum\limits_{K\in T_h} \int_K \frac{\kappa}{2}[(v_h-\psi)_-]^2 dxdy - \sum\limits_{K\in T_h} \int_K \frac{\kappa}{2}[(u_h-\psi)_-]^2 dxdy \geq (f, v_h - u_h), \end{cases} \tag{2.11}$$

where $a_h(w_h, v_h) = \sum\limits_{K\in T_h} \int_K \Delta w_h \Delta v_h + (1-\nu)(2w_{hxy}v_{hxy} - w_{hxx}v_{hyy} - w_{hyy}v_{hxx})]dxdy.$

3. The optimal error estimate

In this section, we will establish error estimates of Bergan's energy-orthogonal FEM for the elastic obstacle problem (1.1) in the energy norm.

Firstly, using the the similar argument to [2], we have

Theorem 3.1. *The problem* (2.11) *is equivalent to the discrete approximation of plate problem:*

$$\begin{cases} \textit{Find } u_h \in V_h, \textit{ such that } \forall v_h \in V_h \\ a_h(u_h, v_h) + \sum\limits_{K\in T_h} \int_K \kappa(u_h-\psi)_- v_h dxdy = (f, v_h), \end{cases} \tag{3.1}$$

which has a unique solution u_h. Moreover, $\|u_h\|_h$ and $\|(u_h-\psi)_-\|_0$ are uniformly bounded independently of h, where $\|\cdot\|_h = (\sum\limits_{K\in T_h} |\cdot|^2_{2,K})^{\frac{1}{2}}$ can be shown to be a norm over V_h by using $(\mathcal{R}1)$ and $(\mathcal{R}2)$ in Lemma 2.1.

In what follows, we will give error estimate for Eq (2.11).

Theorem 3.2. *Assume that u and u_h are the solutions of Eqs* (1.5) *and* (2.11) *respectively, $u \in H^3(\Omega)$ and $f,\ \psi \in L^2(\Omega)$, then we have*

$$\|u - u_h\|_h \leq Ch, \tag{3.2}$$

where the constant C depends on the stiffness of the obstacle κ.

Proof. Since $\|u-u_h\|_h \leq \|u - \Pi_h u\|_h + \|\Pi_h u - u_h\|_h$, in view of Eq (2.9) in $(\mathcal{R}3)$ of Lemma 2.1, we only need to estimate the second term $\|\Pi_h u - u_h\|_h$. In fact, let $w_h = \Pi_h u - u_h$ and employ Eq (3.1), we have

$$\begin{aligned} \|w_h\|_h^2 &\leq C a_h(w_h, w_h) = C\,[a_h(\Pi_h u - u, w_h) + a_h(u, w_h) - a_h(u_h, w_h)] \\ &\leq C\,\|\Pi_h u - u\|_h\,\|w_h\|_h + C\left[a_h(u, w_h) + \sum_{K\in T_h}\int_K \kappa(u_h-\psi)_- w_h dxdy - (f, w_h)\right]. \end{aligned} \tag{3.3}$$

Now we concentrate on the estimate of the second term in the right hand of Eq (3.3). It follows from $(\mathcal{R}1)$ in Lemma 2.1 that $w_h = \bar{w}_h + w_h'$ and there exists a $w \in H^3(K)$ such that

$$w_h|_K = \Pi_K w,\ \bar{w}_h|_K = \bar{r}_K(w),\ w_h'|_K = S_K'(w),\ \int_K \nabla^2 \bar{w}_h : \nabla^2 w_h' dxdy = 0. \tag{3.4}$$

Then we can deduce that

$$\begin{aligned} &a_h(u,w_h)+\sum_{K\in T_h}\int_K \kappa(u_h-\psi)_- w_h dxdy-(f,w_h)\\ &=a_h(u,\bar{w}_h)-(f,\bar{w}_h)+a_h(u,w_h')-(f,w_h')+\sum_{K\in T_h}\int_K \kappa(u_h-\psi)_- w_h dxdy. \end{aligned} \tag{3.5}$$

On one hand, from [2] we know that the solution u of the problem (1.5) satisfies

$$-\int_\Omega \nabla\Delta u\cdot\nabla v dxdy+\int_\Omega \kappa(u-\psi)_- v dxdy=(f,v)\ \ \forall v\in H_0^1(\Omega). \tag{3.6}$$

On the other hand, ($\mathcal{R}2$) in Lemma 2.1 implies $\bar{w}_h \in H_0^1(\Omega)$. Thus applying Green formula and Eq (3.6) yields

$$\begin{aligned} &a_h(u,\bar{w}_h)-(f,\bar{w}_h)\\ &=\sum_{K\in T_h}\int_{\partial K}(\Delta u-(1-\nu)\frac{\partial^2 u}{\partial \mathbf{s}^2})\frac{\partial \bar{w}_h}{\partial \mathbf{n}}ds+(1-\nu)\sum_{K\in T_h}\int_{\partial K}\frac{\partial^2 u}{\partial \mathbf{n}\partial \mathbf{s}}\frac{\partial \bar{w}_h}{\partial \mathbf{s}}ds\\ &\quad-\int_\Omega \nabla(\Delta u)\cdot\nabla\bar{w}_h dxdy-(f,\bar{w}_h)\\ &=\sum_{K\in T_h}\int_{\partial K}(\Delta u-(1-\nu)\frac{\partial^2 u}{\partial \mathbf{s}^2})\frac{\partial \bar{w}_h}{\partial \mathbf{n}}ds+(1-\nu)\sum_{K\in T_h}\int_{\partial K}\frac{\partial^2 u}{\partial \mathbf{n}\partial \mathbf{s}}\frac{\partial \bar{w}_h}{\partial \mathbf{s}}ds-\int_\Omega \kappa(u-\psi)_-\bar{w}_h dxdy, \end{aligned} \tag{3.7}$$

here $\mathbf{n}$ and $\mathbf{s}$ are the unit outward normal vector and tangential vector respectively.

Substituting Eq (3.7) into Eq (3.5) leads to

$$\begin{aligned} &a_h(u,w_h)+\sum_{K\in T_h}\int_K \kappa(u_h-\psi)_- w_h dxdy-(f,w_h)\\ &=\sum_{K\in T_h}\int_{\partial K}(\Delta u-(1-\nu)\frac{\partial^2 u}{\partial \mathbf{s}^2})\frac{\partial \bar{w}_h}{\partial \mathbf{n}}ds+(1-\nu)\sum_{K\in T_h}\int_{\partial K}\frac{\partial^2 u}{\partial \mathbf{n}\partial \mathbf{s}}\frac{\partial \bar{w}_h}{\partial \mathbf{s}}ds+a_h(u,w_h')-(f,w_h')\\ &\quad+\sum_{K\in T_h}\int_K \kappa(u-\psi)_- w_h' dxdy+\sum_{K\in T_h}\int_K \kappa[(u_h-\psi)_- -(u-\psi)_-]w_h dxdy\triangleq\sum_{j=1}^{6}(Er)_j. \end{aligned} \tag{3.8}$$

In what follows, we will estimate $(Er)_j$ one by one for $j=1,2,...,6$.

Firstly, applying Lemmas 3.5 and 3.6 in [21] yields

$$|(Er)_1|\le Ch\|u\|_3\left(\sum_{K\in T_h}\left|\overline{r}_K(w)+r_K'(w)\right|_{2,K}^2\right)^{\frac{1}{2}}. \tag{3.9}$$

By use of Eq (3.4), we get

$$\begin{aligned} &|\overline{r}_K(w)|_{2,K}^2+\left|S'_K(w)\right|_{2,K}^2=|\bar{w}_h|_{2,K}^2+\left|w_h'\right|_{2,K}^2\\ &=\int_K \nabla^2\bar{w}_h:\nabla^2\bar{w}_h dxdy+\int_K \nabla^2 w_h':\nabla^2 w_h' dxdy+2\int_K \nabla^2\bar{w}_h:\nabla^2 w_h' dxdy=|w_h|_{2,K}^2. \end{aligned} \tag{3.10}$$

At the same time, employing Eq (2.10) in ($\mathcal{R}3$) and the inverse estimate gives

$$\left|r'_K(w)\right|_{2,K} \leq Ch_K \left|\Pi_K w\right|_{3,K} \leq C \left|\Pi_K w\right|_{2,K} = C \left|w_h\right|_{2,K}, \tag{3.11}$$

which in conjunction with Eq (3.10) leads to $|(Er)_1| \leq Ch\|u\|_3\|w_h\|_h$.
Secondly, the fact $\bar{w}_h \in H_0^1(\Omega)$ implies $(Er)_2 = 0$.
Thirdly, from Eq (2.2), we have $a_h(\overline{\Pi_h u}, w'_h) = 0$, which together with the Eq (2.10) in ($\mathcal{R}3$) and Eq (3.10) gives

$$|(Er)_3| = |a_h(u - \overline{\Pi_h u}, w'_h)| \leq \|u - \overline{\Pi_h u}\|_h \|w'_h\|_h \leq Ch|u|_3\|w_h\|_h. \tag{3.12}$$

Moreover, it follows from Eq (3.4), Eq (2.10) in ($\mathcal{R}3$) and the inverse estimate that

$$\left|w'_h\right|_{0,K} = \left|S'_K(w)\right|_{0,K} \leq Ch_K^3 \left|\Pi_K w\right|_{3,K} \leq Ch_K^2 \left|\Pi_K w\right|_{2,K} = Ch_K^2 \left|w_h\right|_{2,K}, \tag{3.13}$$

which reveals

$$|(Er)_4| \leq \|f\|_0\|w'_h\|_0 \leq Ch^2\|f\|_0\|w_h\|_h, \tag{3.14}$$

$$|(Er)_5| \leq C \parallel (u-\psi)_- \parallel_0 \|w'_h\|_0 \leq Ch^2 \parallel (u-\psi)_- \parallel_0 \parallel w_h \parallel_h . \tag{3.15}$$

Finally, by use of the elementary inequality $(t_- - s_-)(t - s) \geq 0$ and Theorem 3.1, we have

$$\begin{aligned}
(Er)_6 &= \sum_{K\in T_h} \int_K \kappa[(u_h-\psi)_- - (u-\psi)_-](\Pi_h u - u + u - u_h)dxdy \\
&\leq \sum_{K\in T_h} \int_K \kappa[(u_h-\psi)_- - (u-\psi)_-](\Pi_h u - u)dxdy \\
&\leq C(\parallel (u_h-\psi)_- \parallel_0 + \parallel (u-\psi)_- \parallel_0)\|\Pi_h u - u\|_0 \\
&\leq C \parallel (u-\psi)_- \parallel_0 \|\Pi_h u - u\|_0.
\end{aligned} \tag{3.16}$$

Then combining Eq (3.8) and the above bounds of $(Er)_1$–$(Er)_6$ results in

$$\begin{aligned}
&a_h(u, w_h) + \sum_{K\in T_h} \int_K \kappa(u_h-\psi)_- w_h dxdy - (f, w_h) \\
&\leq Ch(\|u\|_3 + h \parallel f \parallel_0 + h \parallel (u-\psi)_- \parallel_0)\|w_h\|_h + C \parallel (u-\psi)_- \parallel_0 \|\Pi_h u - u\|_0.
\end{aligned} \tag{3.17}$$

Therefore, the desired result Eq (3.2) follows from ($\mathcal{R}3$), Eqs (3.3) and (3.17) immediately. □

Remark. The analysis presented herein is also valid to the elastic obstacle problem (1.1) with $j(v) = \int_\Omega \kappa[(v-\psi)_+]^2 dxdy$, $v_+ = \max\{v, 0\}$ and $f \in L^2(\Omega)$, $f \geq 0$ *a.e. in* Ω.

4. Numerical results

We consider the elastic obstacle problem (1.1) with $\Omega = (0,1)^2$, $f = -10$, $\nu = 0.25$ and an elastic obstacle defined by the function $\psi = \begin{cases} 0 & \text{if } (x,y) \in [0.3, 0.7]^2, \\ -1 & \text{otherwise.} \end{cases}$ The domain Ω is firstly divided into $N \times N$ rectangles. Then each rectangle is further divided along its diagonal into two equal triangles.

Since it is not easy to derive the exact solution, we denote u_N as the N-th level discrete solution and take $\|e_N\|_h = \|u_N - u_{N-1}\|_h$ as the error in the broken energy norm. The numerical results $\|e_N\|_h$ for

different obstacle stiffness parameter $\kappa = 10^j$ $(j = 0, 1, 3, 4)$ with $N = 16, 32, 64, 128$ are given in Table 1 and further plotted in the logarithm scales in Figure 1. We observed that the errors in the energy norm are indeed convergent at optimal order $O(\frac{1}{N})$, i.e., $O(h)$, as $h = \frac{\sqrt{2}}{N} \to 0$. This result is consistent with the theoretical analysis in Theorem 3.2.

Table 1. Numerical results of $\| e_N \|_h$ and Orders under different κ

κ	N	$\| e_N \|_h$	*Order*	κ	N	$\| e_N \|_h$	*Order*
$\kappa = 1$	16	0.1258	–	$\kappa = 10^3$	16	0.1084	–
	32	0.0647	0.9593		32	0.0517	1.0681
	64	0.0326	0.9889		64	0.0259	0.9972
	128	0.0163	1.0000		128	0.0128	1.0168
$\kappa = 10$	16	0.1255	–	$\kappa = 10^4$	16	0.0974	–
	32	0.0645	0.9603		32	0.0402	1.2767
	64	0.0325	0.9889		64	0.0202	0.9928
	128	0.0162	1.0044		128	0.0100	1.0144

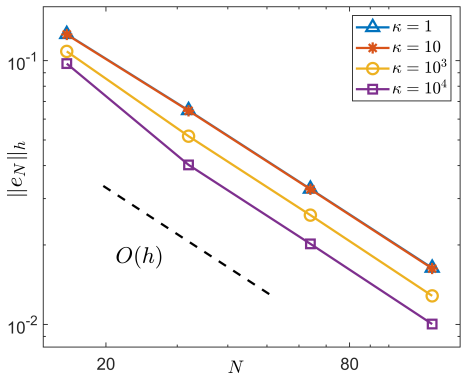

Figure 1. Errors with different parameter κ.

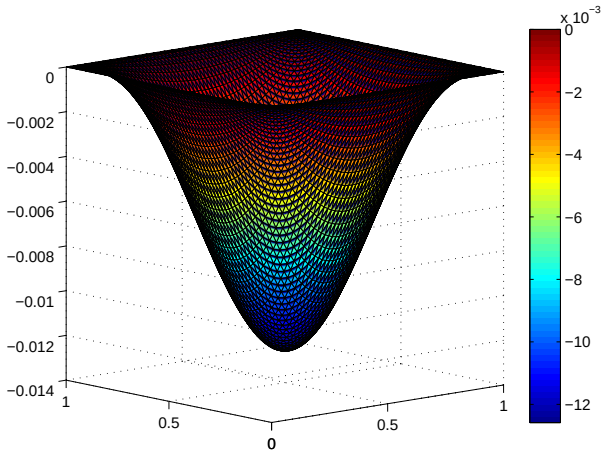

Figure 2. The discrete solution u_N with $\kappa = 1$.

Moreover, the discrete solution u_N with $N = 64$ is also depicted in Figures 2–4, where the parameter κ is chosen as 1, 10^3 and 10^4, respectively. We can see that the bigger parameter κ, the more obvious the influence of obstacles. From Figure 2 ($\kappa = 1$) and Figure 3 ($\kappa = 10^3$), we observe that the difference of κ makes the minimum value of the discrete solution change, but the shape of the solution does not change significantly. In Figure 4 ($\kappa = 10^4$), it is easy to see that the elastic obstacle has a very obvious effect on the solution, which is agrees with the fact that the elastic obstacle will become a rigid obstacle when $\kappa \to \infty$. This phenomenon further indicates the proposed numerical method in this paper can also be used for approximated simulation of the displacement obstacle problem by taking a relatively large obstacle stiffness parameter κ.

In a word, the numerical results in this section confirm the theoretical analysis in Section 3 and indicate the effectiveness of the numerical method.

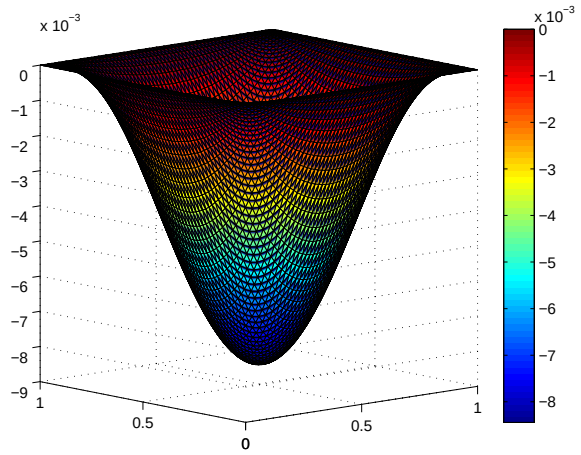

Figure 3. The discrete solution u_N with $\kappa = 10^3$.

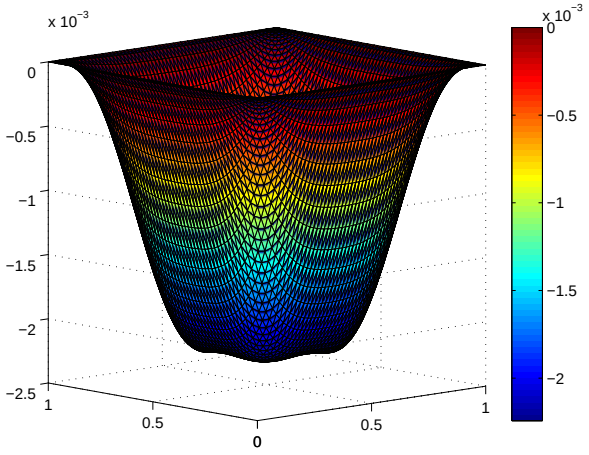

Figure 4. The discrete solution u_N with $\kappa = 10^4$.

Acknowledgements

This work was supported by the National Natural Science Foundation of China (No.11701523, 11801527, 11871441).

Conflict of interest

The authors declare there is no conflict of interest.

References

1. C. Tosone, A. Maceri, The clamped plate with elastic unilateral obstacles: a finite element approach, *Math. Models Meth. Appl. Sci.*, **13** (2003), 1231–1243. https://doi.org/10.1142/S021820250300288X
2. W. M. Han, D. Y. Hua, L. H. Wang, Nonconforming finite element methods for a clamped plate with elastic unilateral obstacle, *J. Integral Equ. Appl.*, **18** (2006), 267–284.
3. R. Glowinski, *Numerical methods for nonlinear variational inequality problems*, New Yrok: Springer-Verlag, 1984.
4. D. Y. Shi, S. C. Chen, Quasi conforming element approximation for a fourth order variational inequality with displacement obstacle, *Acta Math. Sci.*, **23** (2003), 61–66. https://doi.org/10.1016/S0252-9602(17)30146-7
5. D. Y. Shi, S. C. Chen, General estimates on nonconforming elements for a fourth order variational problem, *Numer. Math. Sinica*, **25** (2003), 99–106. https://doi.org/10.1007/s00211-004-0537-6
6. S. C. Brenner, L. Y. Sung, Y. Zhang, Finite element methods for the displacement obstacle problem of clamped plates, *Math. Comput.*, **81** (2012), 1247–1262. https://doi.org/10.1090/S0025-5718-2012-02602-0
7. F. Fang, W. M. Han, J. G. Huang, The virtual element method for an obstacle problem of a Kirchhoff-Love plate, *Commun. Nonlinear Sci. Numer. Simul.*, **103** (2021), 106008. https://doi.org/10.1016/j.cnsns.2021.106008
8. S. C. Brenner, L. Y. Sung, K. N. Wang, Additive Schwarz preconditioners for C^0 interior penalty methods for the obstacle problem of clamped Kirchhoff plates, *Numer. Meth. Part Differ. Equ.*, **38** (2022), 102–117.
9. S. C. Brenner, L. Y. Sung, H. C. Zhang, Y. Zhang, A Morley finite element method for the displacement obstacle problem of clamped Kirchhoff plates, *J. Comput. Appl. Math.*, **254** (2013), 31–42. https://doi.org/10.1016/j.cam.2013.02.028
10. S. C. Brenner, L. Y. Sung, H. C. Zhang, Y. Zhang, A quadratic C^0 interior penalty method for the displacement obstacle problem of clamped Kirchhoff plates, *SIAM J. Numer. Anal.*, **50** (2012), 3329–3350. https://doi.org/10.1137/110845926
11. D. Y. Shi, L. F. Pei, Double set parameter finite element method for two-sided displacement obstacle problem of clamped plate, *J. Math. Anal. Appl.*, **436** (2016), 203–216. https://doi.org/10.1016/j.jmaa.2015.11.004

12. D. Y. Shi, L. F. Pei, A new error analysis of Bergan's energy-orthogonal element for two-sided displacement obstacle problem of clamped plate, *J. Math. Anal. Appl.*, **442** (2016), 339–352. https://doi.org/10.1016/j.jmaa.2016.04.058
13. W. B. Liu, W. Gong, N. N. Yan, A new finite element approximation of a state-constrained optimal control problem, *J. Comput. Math.,* **27** (2009), 97–114.
14. W. Gong, N. N. Yan, Mixed finite element scheme for optimal control problems with pointwise state constraints, *J. Sci. Comput.*, **46** (2011), 182–203. https://doi.org/10.1007/s10915-010-9392-z
15. J. L. Qiu, J. K. Zhao, F. Wang, Nonconforming virtual element methods for the fourth-order variational inequalities of the first kind, *J. Comput. Appl. Math.*, **425** (2023), 115025. https://doi.org/10.1016/j.cam.2022.115025
16. J. T. Cui, Y. Zhang, A new analysis of discontinuous Galerkin methods for a fourth order variational inequality, *Comput. Meth. Appl. Mech. Eng.*, **1** (2019), 531–547.
17. F. Wang, J. K. Zhao, Conforming and nonconforming virtual element methods for a Kirchhoff plate contact problem, *IMA J Numer. Anal.*, **41** (2021), 1496–1521. https://doi.org/10.1093/imanum/draa005
18. T. Gustafsson, R. Stenberg, J. Videman, A stabilized finite element method for the plate obstacle problem, *BIT Numer. Math.*, **59** (2018), 97–124. https://doi.org/10.1016/0045-7825(87)90001-6
19. C. A. Felippa, P. G. Bergan, A triangular bending element based on energy-orthogonal free formulation, *Comput. Meth. Appl. Mech. Eng.*, **61** (1987), 129–160. https://doi.org/10.1016/0045-7825(87)90001-6
20. Z. C. Shi, S. C. Chen, F. Zhang, Convergence analysis of Bergan's energy-orthogonal plate element, *Math. Models Meth. Appl. Sci.*, **4** (1994), 489–507. https://doi.org/10.1142/S0218202594000285
21. Z. C. Shi, Convergence of the TRUNC plate element, *Comput. Meth. Appl. Mech. Eng.*, **62** (1987), 71–88. https://doi.org/10.1016/0045-7825(87)90090-9

AIMS Press